Robust Anti-Jamming Beamforming Scheme for Cellular-Connected Mobile UAV

Jiajia Huang, Ernest Kurniawan, Sumei Sun
Institute for Infocomm Research (I2R), Agency for Science, Technology and Research (A*STAR), Singapore
Email: {huang_jiajia, ekurniawan, sunsm}@i2r.a-star.edu.sg

***Abstract*—Beamforming is a promising anti-jamming technique for cellular-connected unmanned aerial vehicle (UAV) system. It is challenging to design anti-jamming beamforming vectors for moving UAV with imperfect CSI. In this paper, we consider an uplink transmission from UAV to multi-antenna ground base station (BS) in the presence of a malicious ground jammer. We propose a deep learning based beamforming network (DLBF) to maximize the average data rate for moving UAV in the presence of a ground jammer. Complexity analysis shows that DLBF has linear complexity, which indicates good scalability in large antenna arrays. Extensive simulation results show that anti-jamming DLBF improves average data rate for moving UAV. The performance of DLBF advantage is robust under imperfect CSI and different antenna configurations.**

***Index Terms*—Deep learning, beamforming, unmanned aerial vehicle (UAV)**

I. Introduction

To achieve ubiquitous connectivity in the fifth generation (5G) and beyond 5G network, cellular-connected unmanned aerial vehicles (UAVs) have emerged to be one promising solution due to their mobility and flexibility. By integrating UAVs into future cellular network, a plethora of applications such as video streaming, surveillance, and drone delivery could be enabled. The UAV to ground base station channel, while enjoying the benefit brought by line-of-sight (LoS) characteristics of the air-to-ground (A2G) channel, is vulnerable to the threat of jamming attacks [1].

Classical anti-jamming techniques such as frequency hopping and spread spectrum leads to inefficient channel utilization and thus will not be able to support high speed data transmission requirements in the UAV applications [2].

With the development of antenna array technology, beamforming-based physical layer security enhancement mechanism has attracted a lot of research attention [3]–[7]. Conventional beamforming techniques such as maximal ratio combining (MRC), zero-forcing (ZF), and minimum mean square error (MMSE) based beamformer can be used [8]. MRC focuses on maximizing the desired signal. But it fails to mitigate the jamming signal. ZF aims to null the jamming signal. MMSE based receiver is designed to minimize the MMSE between the desired signal and filtered signal. ZF, MMSE are able to provide certain anti-jamming functionality with the assumption of perfect global channel state information (CSI). However, their performance could be severely degraded with imperfect CSI. It is hard to acquire perfect CSI in practice, especially for the unknown and non-cooperative jammer. Minimum variance distortionless response (MVDR) and its variants are more adaptive algorithms [4], [5]. MVDR is designed to minimize the variance of the residual noise at the output while passing the desired signal without distortion. MMSE and MVDR based beamformers involve high complexity matrix inversion, limiting their scalability to large antenna arrays. In more recent years, there are works which propose to solve anti-jamming problem with the aid of intelligent reflecting surfaces (IRS) [6]. For example, the authors in [6] proposed to utilize IRS with beamforming to enhance anti-jamming performance for the downlink transmission from the BS to multiple ground IoT users. Although promising, the cost of setting up extra IRS in the system is still high.

Deep learning (DL) technology has great potential in solving complex beamforming design problems. DL method usually has lower complexity during online inference stage and can be more efficient with parrallel computing accelaration using graphical processing unit (GPU). Moreover, through extensive training, DL methods are expected to have better robustness to imperfect CSI. There are some research attempts in this area [9], [10]. In [9], the authors presented deep learning based beamforming neural network (BFNN) for downlink transmission to maximize spectral efficiency with imperfect CSI. They considered a multiple-input single-output (MISO) system without a jammer. In [10], the authors proposed a deep learning based 3D robust beamforming to maximize secrecy rate for downlink UAV system with the existence of a eavesdropper. This work mainly considers passive eavesdropper, and assumes the UAV location is known and fixed.

In this paper, we propose a scalable and robust deep learning based beamforming (DLBF) algorithm for anti-jamming in cellular-connected UAV network. The main contributions of our work can be summarized as follows,

- We propose a deep learning based anti-jamming beamforming design for multi-antenna ground base station (BS), aiming to enhance desired signals from moving UAV, and mitigate jamming signal from a ground jammer.
- The proposed DLBF algorithm is robust against imperfect CSI.
- Complexity analysis shows that the proposed algorithm has good scalibility as number of antennas increase.
- Extensive simulations are conducted to evaluate the performance of the proposed DLBF algorithm under perfect and imperfect CSI, and in different antenna configurations.

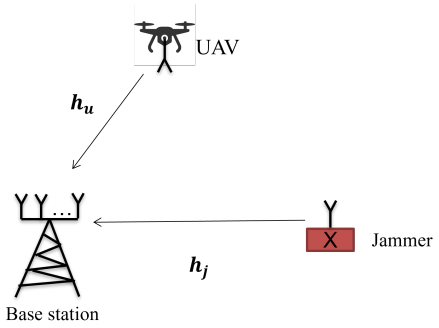

Figure 1: System model.

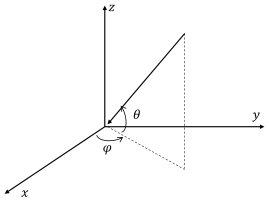

Figure 2: Azimuth AOA and elevation AOA.

The rest of the paper is organized as follows. Section II establishes the system model for analyzing the uplink transmission from UAV to ground BS and gives the problem formulation. Section III presents the design of the DLBF network structure as well as the complexity analysis. Section IV evaluates the performance of the proposed algorithm. Section V concludes this paper.

II. System Model and Problem Statement

As shown in Fig. 1, the system consists of one ground base station equipped with $N_h \times N_v$ uniform planer array (UPA), where N_h is the number of antennas along the horizontal direction, and N_v denotes the number of antennas along the vertical direction. The UPA enables 3-dimensional (3D) beamforming capability at the BS, such that the BS can serve users from the sky while rejecting jamming signals from the ground. The legitimate user UAV and the ground jammer are equipped with single antenna. We consider a flying UAV aiming to send data back to the BS, during transmission, the ground jammer emits jamming signal to disrupt the legitimate uplink transmission. The legitimate communication could be severely disrupted without proper protection design. Consequently, we aim to design receive beamforming vector at the BS to suppress jamming signal and enhance the desired signal.

A. Channel Model

The following subsection presents the channel model. This work considers narrow-band transmission. Our proposed method can be extended in a straightforward manner to wideband frequency selective fading channels with orthogonal frequency division multiplexing (OFDM).

1) UAV to BS channel: The uplink channel between the UAV and BS is denoted as $\mathbf{h}_u \in \mathbb{C}^{N_b \times 1}$, $N_b = N_h N_v$. the channel between jammer to BS is denoted as $\mathbf{h}_j \in \mathbb{C}^{N_b \times 1}$. The UAV to BS channel model follows the air-to-ground (A2G) channel model where large scale path loss fading and small-scale Rician fading are considered.

As for small scale fading, Rician fading is used to model both line-of-sight (LOS) and non-line-of-sight (NLOS) component, which can be described as follows [10].

$$\mathbf{h}_u = \sqrt{\frac{K}{1+K}}\mathbf{h}_{uL} + \sqrt{\frac{1}{1+K}}\mathbf{h}_{uN}, \tag{1}$$

where

- K is the Rician factor
- $\mathbf{h}_{uN}$ is the NLOS component of the UAV to BS channel, whose entries are assumed to follow independent and identical distributed (i.i.d.) circularly symmetric complex Gaussian distribution
- $\mathbf{h}_{uL}$ is the LOS component, which can be expressed in terms of receiver and transmitter steering vector as follows.

$$\mathbf{h}_{uL} = \mathbf{a}_r \mathbf{a}_t \tag{2}$$

where $\mathbf{a}_r$ is the steering vector of the receiver (the BS), $\mathbf{a}_t$ is the steering vector of the transmitter (UAV). The BS has UPA antenna, hence, the $N_b \times 1$ steering vector $\mathbf{a}_r$ is a function of the azimuth angle-of-arrival (AOA) φ_u and the elevation AOA θ_u. In this paper, the elevation AOA θ and azimuth AOA φ are defined as in Figure 2. The k-th entry of $\mathbf{a}_r$ can be written as follows.

$$a_r^k = e^{-j\frac{2\pi}{\lambda_c}\delta_u[(n_h-1)\cos\theta_u\cos\varphi_u + (n_v-1)\sin\theta_u]}, \tag{3}$$

where λ_c is wavelength of the center frequency. δ_u is the antenna spacing at the base station, we assume the vertical and horizontal antenna spacing are the same. $n_v = 1, .., N_v$ is the antenna element position in the vertical direction, $n_h = 1, ..., N_h$ is the antenna element position in the horizontal direction, $k = N_h(n_v - 1) + n_h$. As for transmitter steering vector, since the UAV has only one antenna, $\mathbf{a}_t = 1$.

To model the imperfect channel state information (CSI), we assume that $\mathbf{h}_{uL}$ can be determined once the location of the UAV is known [11]. And assume the error comes from the NLOS component, the imperfect NLOS part $\hat{\mathbf{h}}_{uN}$ can be modeled as follows,

$$\hat{\mathbf{h}}_{uN} = \sqrt{\alpha_u}\mathbf{h}_{uN} + \sqrt{1-\alpha_u}\boldsymbol{\epsilon}_{uN} \tag{4}$$

where α_u is the CSI knowledge factor, $\mathbf{h}_{uN}$ is the actual NLOS component, $\boldsymbol{\epsilon}_{uN}$ is the estimation error whose entries follow independent and identically distributed (i.i.d) Gaussian distribution. With this, the overall channel model for UAV to BS, in the presence of the imperfect CSI, could be written as,

$$\hat{\mathbf{h}}_u = \sqrt{\frac{K}{1+K}}\mathbf{h}_{uL} + \sqrt{\frac{1}{1+K}}\hat{\mathbf{h}}_{uN} \tag{5}$$

2) Jammer to BS channel: The jammer to BS channel is a typical ground-to-ground(G2G) channel, which can be modeled as [12],

$$\mathbf{h}_j = \sum_{l=1}^{L} A_l \mathbf{a}_r(\theta_j^l, \varphi_j^l), \tag{6}$$

where A_l denotes the complex gain of the l-th path, $\mathbf{a}_r(\theta_j^l, \varphi_j^l)$ denotes the antenna array response vector of the jamming signal at the BS, with φ_j^l denotes the azimuth AOA of the jamming signal from the l-th path, θ_j^l denotes the elevation AOA of the jamming signal from the l-th path. $l = 1$ denotes the LOS path, and $l > 1$ denote the NLOS paths. Similarly, we model the imperfect CSI with similar model as for UAV-BS. First, we rewrite the jammer-BS channel as the LOS and NLOS part,

$$\mathbf{h}_j = \mathbf{h}_{jL} + \mathbf{h}_{jN}, \tag{7}$$

where $\mathbf{h}_{jL} = A_1 \mathbf{a}_r(\theta_j^1, \varphi_j^1)$, and $\mathbf{h}_{jN} = \sum_{l=2}^{L} A_l \mathbf{a}_r(\theta_j^l, \varphi_j^l)$. Then, the imperfect jammer-BS channel estimation is modeled as,

$$\hat{\mathbf{h}}_j = \mathbf{h}_{jL} + \hat{\mathbf{h}}_{jN}, \tag{8}$$

where $\hat{\mathbf{h}}_{jN} = \sqrt{\alpha_j}\mathbf{h}_{jN} + \sqrt{1-\alpha_j}\boldsymbol{\epsilon}_{jN}$. α_j is the CSI knowledge factor of the jammer to BS channel. $\mathbf{h}_{jN}$ is the actual NLOS component. $\boldsymbol{\epsilon}_{jN}$ is the estimation error, whose entries follow i.i.d Gaussian distribution.

3) Receive Signal: With the above established channel model, the received signal at the BS can be given as,

$$\mathbf{y} = \mathbf{h}_u s_u + \mathbf{h}_j s_j + \mathbf{n}, \tag{9}$$

where $\mathbf{y} \in \mathbb{C}^{N_b \times 1}$ is the received signal at the BS, $\mathbf{h}_u \in \mathbb{C}^{N_b \times 1}$ is the UAV-BS channel coefficient matrix, $\mathbf{h}_j \in \mathbb{C}^{N_b \times 1}$ is the jammer-BS channel coefficient matrix, s_u denotes the transmit symbol from the UAV, s_j denotes the transmit symbol from the jammer, $\mathbf{n} \in \mathbb{C}^{N_b \times 1}$ is the additive Gaussian Noise.

Since the BS is equipped with UPA, the received signal will be processed by the receive beamforming vector $\mathbf{v}$, to obtain a beamformed received signal, as follows

$$\begin{aligned} \tilde{\mathbf{y}} &= \mathbf{v}^H \mathbf{y} \\ &= \mathbf{v}^H \mathbf{h}_u s_u + \mathbf{v}^H \mathbf{h}_j s_j + \mathbf{v}^H \mathbf{n}, \end{aligned} \tag{10}$$

where $\mathbf{v} \in \mathbb{C}^{N_b \times 1}$ is the beamforming vector at the BS, $\{\cdot\}^H$ denotes the conjugate transpose.

The SINR at BS is given as,

$$\gamma = \frac{\left|\mathbf{v}^H \mathbf{h}_u\right|^2}{\left|\mathbf{v}^H \mathbf{h}_j\right|^2 + \left|\mathbf{v}^H \mathbf{n}\right|^2} \tag{11}$$

B. Problem Formulation

Our objective is to enhance the desired signal from the UAV and mitigate the jamming signal from the ground, by properly designing the beamforming vector at the BS. Formally, the problem can be formulated as the following optimization problem, with the objective to maximize the system rate, with the constraints on beamforming vector.

$$\begin{aligned} \max_{\mathbf{v}} \quad & \log_2(1+\gamma) \\ \text{s.t.} \quad & |\mathbf{v}|^2 = 1 \end{aligned} \tag{12}$$

It is challenging to solve the optimization problem (12), because the objective function is non-convex with respect to receive beamforming vector $\mathbf{v}$. Moreover, the imperfect CSI models further complicate the problem.

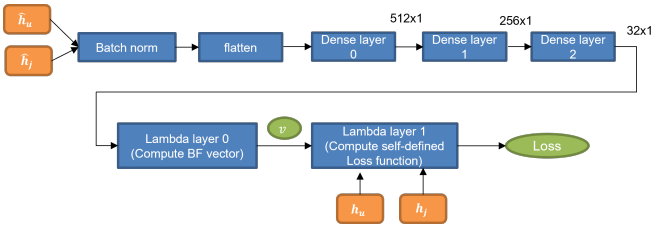

Figure 3: Training with custom defined loss function.

III. Deep Learning Based Beamforming (DLBF) Design

Leveraging the ability of neural networks to solve complex problem, in this section, we propose to optimize the receive beamforming vector by a deep learning beamforming (DLBF) network. The detail of network layers and the complexity analysis are presented in the following.

A. DLBF Network Architecture

Figure 3 shows the DLBF network architecture, the DLBF network consists of 3 dense layers, and 2 specially designed Lambda layers. The 3 dense layers are used to extract the features from the imperfect CSI input, the first Lambda layer is designed to generate complex beamforming vector, the second Lambda layer is used to compute custom loss function.

1) Lambda Layer 0: This layer is a custom layer to output a complex-valued, unit-norm beamforming vector. Specifically, the desired beamforming vector $\mathbf{v}$ is a $N_b \times 1$ complex-valued vector. Since the dense layer is only capable to output real-values. The last dense layer is designed to output $2N_b$ real values. The first N_b real values will be used for the real part of the beamforming vector, $\mathbf{v}_{re}$, and the following N_b real values will be used for the imaginary part of the beamforming vector $\mathbf{v}_{im}$. Then the final beamforming vector is obtained by adding the real and imaginary parts as follows,

$$\mathbf{v} = \mathbf{v}_{re} + j\mathbf{v}_{im}. \tag{13}$$

2) Lambda Layer 1: This layer is another custom layer to compute custom loss function. Since the objective is to maximize the system rate, the loss function is designed to be directly related to objective function in (12), which can be described as,

$$\text{Loss} = -\frac{1}{M}\sum_{m=1}^{M} \log_2(1+\gamma_m), \tag{14}$$

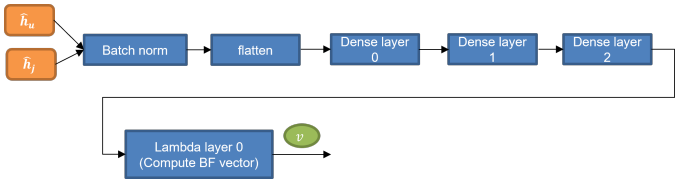

Figure 4: Online deployment and inference.

where M is the training batch size, and γ_m denotes the SINR of the m-th sample. When computing γ_m, the perfect CSI will be used. During training, minimizing the loss via back propagation will increase the system rate. One thing to note is that, perfect CSI is only needed for offline training. For deployment and online inference, only imperfect CSI is needed.

B. DLBF Offline Training and Online Inference

During the training of the DLBF, both perfect CSI and imperfect CSI will be used at different stage of the training. The imperfect CSI $\hat{\mathbf{h}}_u$ and $\hat{\mathbf{h}}_j$ will be normalized and feed into the dense layers. The dense layers will extract the channel characteristic in the imperfect CSI. After feature extraction, the output of the dense layer will be fed to Lambda layer 0 to compute the beamforming vector. Intuitively, in the offline training, the DLBF learns to generate a receive beamforming vector based on features extracted from imperfect CSI, aiming to minimize loss function computed with perfect CSI. In other words, the use of perfect CSI in the loss function guides the beamforming design to approach the ideal system rate as much as possible with perfect CSI and to be robust to channel estimation error. During the offline training stage, the perfect CSI of the jammer can be obtained by using a legitimate transmitter known to the BS that mimics the role of a jammer.

At the online deployment stage, as shown in Figure 4, the DLBF will take the imperfect CSI as input and generate the suggested beamforming vector as output without the need to know perfect CSI. The imperfect CSI of jammer can be obtained by blind estimation algorithms [13].

The structure parameters of DLBF network implemented in this paper is given by Table I. It is worth noting that the DLBF network structure is dependent on the number of antennas N_b. More specifically, the input dimension of the first dense layer, the output dimension of the third dense layer as well as the Lambda Layer 0 depend on the number of antennas at the BS. When the number of antenna changes, the network structure should be changed accordingly.

C. Complexity Analysis

We analyze the complexity of the proposed DLBF using the number of floating point operations (FLOPs) as the measure for complexity. For DLBF, we only count the complexity for online deployment stage. The complexity of online inference stage mainly comes from the dense layers. The FLOPs of the dense layer can be given by $(2N_I - 1)N_O$ [14], where N_I is the input dimensions, and N_O is the output dimensions.

Table I: DLBF implementation details.

Layer	Output Dim.	Activation Func.
Input Layer	$2N_b \times 1$	N.A.
Dense Layer	512×1	Relu
Dense Layer	256×1	Relu
Dense Layer	$2N_b \times 1$	Relu
Lambda Layer 0	$N_b \times 1$	N.A.
Lambda Layer 1	1	N.A.

Table II: Simulation parameters.

Parameter	Value
center frequency, f_c	3.2 GHz
antenna spacing, δ_u	$\frac{1}{2}\lambda_c$
noise power, σ_n^2	-90 dBm
Rician factor, K	1

Consider the DLBF network structure given in Table I, the total number of FLOPs can be expressed as $C_1 N_b + C_2$, where $C_1 = 4c_1 + 4c_2 - 2$, and $C_2 = 2c_1c_2 - c_2 - c_1$, where c_1, c_2 are the output dimension of dense layer 1 and 2. It can be observed that DLBF's computation complexity grows linearly as number of antenna grows, suggesting good scalability.

IV. Performance Evaluation

A. Dataset Generation

The training and testing data samples are generated using Matlab following the models defined in (1) - (7). Specifically, the perfect CSIs are generated following the definition in (1) and (7), the imperfect CSIs are generated following the definition in (5) and (8). The corresponding parameters are listed in Table II. In our simulation, we assume that the UAV is flying in the region that is defined by $x \geq 0, y \geq 0, z \geq 0$, and the jammer on the ground, which is located in the same xy plane as the BS. The training samples covers all possible AoAs, and the testing samples consists of CSI samples that are generated with AoAs randomly selected in the feasible regions. $200,000$ samples are used for training, and $100,000$ samples are generated for testing.

B. Results

We define the relative received SNR as the ratio between the received power from UAV and the noise power, $\text{SNR}_r = \frac{P_u}{\sigma_n^2}$. In the following, we evaluate the performance of DLBF by varying the number of antennas and relative SNR. Four conventional receive beamforming algorithms are selected as benchmarks: MRC, ZF, MMSE [8] and MVDR [3].

1) Robustness to Imperfect CSI: Fig. 5 shows the average system rate comparison under various imperfect CSI conditions. 4×4 UPA antenna are used, relative SNR is set to 2 dB. In Fig. 5a, we keep $\alpha_j = 0.3$ and vary α_u from 0.1 to 1. Lower α_u means worse CSI knowledge from the UAV. It

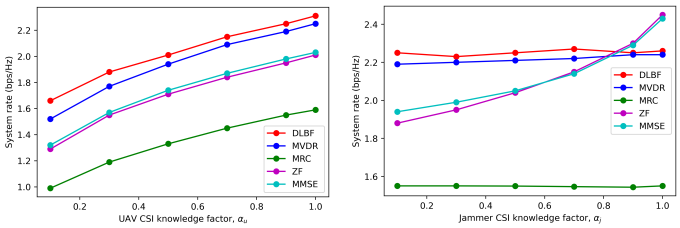

(a) Varying UAV CSI. (b) Varying jammer CSI.

Figure 5: Performance comparison under different CSI knowledge.

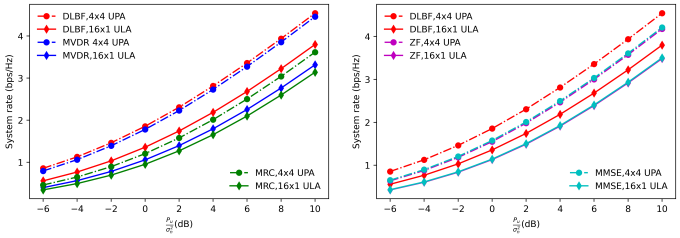

Figure 6: Performance comparison with different antenna type.

can be observed that the proposed DLBF outperforms all the benchmark algorithms, even when the CSI knowledge from the UAV is poor. Specifically, when $\alpha_u = 0.1$, DLBF outperforms MVDR, ZF, MMSE, MRC by $9\%, 26\%, 27\%, 68\%$, respectively. This shows the advantage of DLBF under imperfect CSI condition, especially with poor CSI knowledge. In Fig. 5b, we keep $\alpha_u = 0.9$, and vary α_j from 0.1 to 1. It can be observed that the average rates of DLBF, MVDR, and MRC remain relatively constant as the jammer CSI knowledge changes. While the performance of ZF and MMSE are quite sensitive the the change of α_j. For instance, when the jammer CSI is close to perfect ($\alpha_j \geq 0.9$), ZF and MMSE achieve better rates than DLBF. However, when the CSI knowledge from the jammer is poor (e.g. $\alpha_j = 0.1$), their performance drops significantly (36%). And it is worth noting that nearly perfect CSI knowledge is hard to obtain in practice, especially for the unknown jammer.

2) Impact of Antenna Type: Fig. 6 shows the performance comparison for UPA and uniform linear array (ULA). All algorithms are evaluated with imperfect CSI, where $\alpha_u = 0.95, \alpha_j = 0.3$. It can be observed that given the same number of antennas, configuring the antennas in UPA gives better performance than ULA for all algorithms. For example, when relative SNR is 2 dB, DLBF with 4×4 UPA achieves 32% improvement in data rate compared to DLBF with 16×1 ULA. The reason is that UPA has better beamfoming flexibility in 3D dimension, while ULA is mainly used for 2D beamforming. Additionally, DLBF with ULA constantly outperforms other benchmarks across different relative SNRs. Specifically, DLBF with ULA outperforms MVDR with ULA by 24% given the same number of antennas.

V. Concluding Remarks

In this paper, we proposed a robust DLBF algorithm for anti-jamming in cellular-connected UAV networks. Extensive simulation results show that our proposed DLBF algorithm maintains good system rate with imperfect CSI, validating its robustness to channel imperfection. Complexity analysis shows that the complexity of DLBF grows linearly with number of antennas, indicating that DLBF has good scalability and is suitable for large antenna arrays. Additionally, DLBF outperforms other benchmarks in both UPA and ULA antenna configuration.

Acknowledgment

This work is supported by the NRF, Singapore and IMDA under its Future Communications R&D Programme, and by the A*STAR 5G-AMSUS-WP1 project.

References

[1] A. Fotouhi, H. Qiang, M. Ding, M. Hassan, L. G. Giordano, A. Garcia-Rodriguez, and J. Yuan, "Survey on uav cellular communications: Practical aspects, standardization advancements, regulation, and security challenges," *IEEE Communications surveys & tutorials*, vol. 21, no. 4, pp. 3417–3442, 2019.

[2] J. Peng, Z. Zhang, Q. Wu, and B. Zhang, "Anti-jamming communications in uav swarms: A reinforcement learning approach," *IEEE Access*, vol. 7, pp. 180 532–180 543, 2019.

[3] C. Pan, J. Chen, and J. Benesty, "Performance study of the mvdr beamformer as a function of the source incidence angle," *IEEE/ACM Transactions on Audio, Speech, and Language Processing*, vol. 22, no. 1, pp. 67–79, 2013.

[4] L. Zhang, L. Huang, B. Li, M. Huang, J. Yin, and W. Bao, "Fast-moving jamming suppression for uav navigation: A minimum dispersion distortionless response beamforming approach," *IEEE Transactions on Vehicular Technology*, vol. 68, no. 8, pp. 7815–7827, 2019.

[5] X. Dai, J. Nie, F. Chen, and G. Ou, "Distortionless space-time adaptive processor based on mvdr beamformer for gnss receiver," *IET Radar, Sonar & Navigation*, vol. 11, no. 10, pp. 1488–1494, 2017.

[6] Y. Sun, K. An, J. Luo, Y. Zhu, G. Zheng, and S. Chatzinotas, "Outage constrained robust beamforming optimization for multiuser irs-assisted anti-jamming communications with incomplete information," *IEEE Internet of Things Journal*, 2022.

[7] H. Zhao, J. Hao, and Y. Guo, "Joint trajectory and beamforming design for irs-assisted anti-jamming uav communication," in *2022 IEEE Wireless Communications and Networking Conference (WCNC)*. IEEE, 2022, pp. 369–374.

[8] T. T. Do, E. Björnson, E. G. Larsson, and S. M. Razavizadeh, "Jamming-resistant receivers for the massive mimo uplink," *IEEE Transactions on Information Forensics and Security*, vol. 13, no. 1, pp. 210–223, 2017.

[9] T. Lin and Y. Zhu, "Beamforming design for large-scale antenna arrays using deep learning," *IEEE Wireless Communications Letters*, vol. 9, no. 1, pp. 103–107, 2019.

[10] R. Dong, B. Wang, and K. Cao, "Deep Learning Driven 3D Robust Beamforming for Secure Communication of UAV Systems," *IEEE Wireless Communications Letters*, vol. 10, no. 8, pp. 1643–1647, Aug. 2021, conference Name: IEEE Wireless Communications Letters.

[11] H. Yang, K.-Y. Lam, J. Nie, J. Zhao, S. Garg, L. Xiao, Z. Xiong, and M. Guizani, "3D Beamforming Based on Deep Learning for Secure Communication in 5G and Beyond Wireless Networks," in *2021 IEEE Globecom Workshops (GC Wkshps)*. Madrid, Spain: IEEE, Dec. 2021, pp. 1–6.

[12] T. Lin and Y. Zhu, "Beamforming design for large-scale antenna arrays using deep learning," *IEEE Wireless Communications Letters*, vol. 9, no. 1, pp. 103–107, 2019, publisher: IEEE.

[13] S. Ma, G. Wang, R. Fan, and C. Tellambura, "Blind channel estimation for ambient backscatter communication systems," *IEEE Communications letters*, vol. 22, no. 6, pp. 1296–1299, 2018.

[14] P. Molchanov, S. Tyree, T. Karras, T. Aila, and J. Kautz, "Pruning convolutional neural networks for resource efficient inference," *arXiv preprint arXiv:1611.06440*, 2016.